

# A Unified Analytical Approach to Multi-Cell LBT-Based Spectrum Sharing Systems

Yao Ma, Susanna Mosleh, and Jason Coder

CTL, National Institute of Standards and Technology

325 Broadway, Boulder, Colorado, USA

**Abstract**— Future unlicensed spectrum sharing scenarios involve multi-cell, multi-tier access of incumbent and emerging wireless systems, such as wireless local area network (WLAN), New-Radio unlicensed (NR-U), and Long-Term Evolution (LTE) with Licensed-Assisted Access (LAA). Listen-before-talk (LBT) medium access control (MAC) is a common technique used for channel sensing and access control. Despite intense research efforts, the majority of available results have not accurately analyzed multi-cell LBT with imperfect spectrum sensing. Furthermore, while past studies involved two major spectrum sharing strategies – shared cell access (SCA) and exclusive cell access (ECA), they missed a systematic comparison between the two. In this paper, we develop a unified analytical approach which maps the effects of imperfect spectrum sensing and multi-cell, multi-tier LBT to the key performance indicators (KPIs) of LAA and WLAN cells. We provide an analytical comparison between the SCA and ECA schemes, and show that the SCA can provide a significantly higher system throughput than the ECA as a function of sensing thresholds. We program the SCA and ECA algorithms with a new simulation method and implement Monte Carlo simulations, which verify our analytical results. Numerical results provide insightful observations on effects of various parameters. These results provide powerful analytical and simulation tools to evaluate the performance of multi-tier LBT coexistence systems with imperfect sensing, and effectively support coexistence system optimization.

Index Terms: Imperfect spectrum sensing, LTE-LAA, Multi-tier coexistence, Multi-cell LBT, WLAN.

## I. INTRODUCTION

Spectrum sharing in heterogeneous 4G and 5G wireless systems [1]–[4] involves multiple radio access technologies (RATs) of emerging wireless systems such as cellular Long-Term Evolution (LTE) or New Radio (NR) systems with unlicensed or License Assisted Access (LAA) [1]–[3], and incumbent services such as wireless local area networks (WLANs) [5], [6]. In these systems, various listen-before-talk (LBT) medium access control (MAC) schemes are used for channel sensing and access control.

Regarding LBT-based multi-cell spectrum sharing, there are two popular assumptions or schemes which we call shared cell access (SCA) and exclusive cell access (ECA), respectively. Both schemes use clear channel assessment (CCA) and detect the channel busy/idle states of adjacent cells. Without loss of generality, we assume that each LAA small-cell base station (SBS) or WLAN access point (AP) does the sensing, and schedules downlink transmissions in each cell (or contention zone).

In the SCA model, each SBS/AP assumes imperfect sensing and can schedule transmissions when the received intercell interference (ICI) from adjacent cells is below the sensing threshold. This model allows several cells (or links) to transmit simultaneously when the mutual ICIs are below their sensing thresholds. The SCA methods for multi-cell networks have been considered in [7]–[10], to name a few.

The ECA scheme assumes that at any time a successful transmission happens when only one link is transmitting. It is consistent with the carrier sense multiple access with collision avoidance (CSMA/CA) performance modeling provided in [11]. The ECA scheme has been assumed in [12]–[16] for spectrum sharing. Certainly, the ECA scheme applies only to a small area of highly overlapped cells, when the SBS/AP sensing thresholds are set to be adequately low. The ECA scheme can be regarded as a special case of the SCA scheme.

In the studies mentioned above, the effect of ICI sensing errors on the network throughput has not been explicitly addressed. Furthermore, the LBT MAC features for the SCA have not been adequately modeled or studied. For example, [7], [8], [12] did not model an important MAC metric – average channel busy time to support a successful transmission. The effect of inter-SBS/AP ICI sensing errors was only implicitly studied in [12], and the LBT MAC feature (such as multistage backoff) was not adequately modeled. We have provided a novel analytical approach to evaluate the effect of CCA errors on the LAA and WLAN network throughput in [17] assuming an ECA scheme. The result in [17] cannot be readily applied to the SCA scheme.

In summary, analyzing the effect of CCA errors on the key performance indicators (KPIs) of multi-cell LBT coexistence systems has not been satisfactorily addressed in the literature. Furthermore, there is a lack of a systematic comparison of SCA and ECA models in a unified framework. It is interesting to investigate if the SCA can provide higher KPIs than the ECA even when cells are densely overlapped. Yet we could not find such a comparative analysis available in the literature. This comparative analysis is useful, for example, on the selection of sensing threshold and MAC parameters, and the design of better spectrum sharing algorithms.

The related computer simulation work is non-trivial, because the traditional discrete-event driven simulation methods, such as those targeted for the ECA (in [11], [15]) and/or perfect channel sensing, cannot be directly used. The imperfect sensing in a multi-cell network can cause multiple nodes to implement backoff or transmission simultaneously. The sim-

\*U.S. Government work, not subject to U.S. copyright.

ulation shall model the resulting mis-detection and collision events in a fine time step-size of a CCA duration, and follow the multicell LBT procedure. We are not aware of an open-source or commercial software that can readily simulate such a scenario.

In this paper, we address the challenging problem of modeling and analysis for multi-cell LAA and WLAN coexistence networks with imperfect sensing of ICIs, and treat the SCA and ECA schemes in a unified framework. We highlight the novel contributions as follows:

- We develop a new method on integrating effects of spectrum sensing detection probability and multi-cell LBT MAC features, and mapping them to the system KPIs, including the channel access probability (CAP), successful transmission probability (STP), and throughput.
- We provide a unified analysis and systematic comparison of the SCA and ECA schemes for LAA and WLAN coexistence networks.
- By developing a new simulation method, we program the SCA and ECA algorithms with multi-cell and multi-tier LBT, and implement Monte Carlo simulations, which validate our analytical results.

Numerical results show the effects of critical MAC and physical layer parameters such as sensing threshold and detection probability, and demonstrate the performance improvement of the SCA scheme over the ECA scheme. This technique provides significant progress on performance modeling and analysis of multi-cell LBT coexistence schemes, and support 4G and 5G multi-cell optimization in license-assisted or unlicensed spectrum bands.

## II. SYSTEM MODEL

We consider a two-tier channel access system on a 5 GHz industrial, scientific, and medical (ISM) radio band, where there is an LTE-LAA system with  $C_L$  small cells and a WLAN system with  $C_W$  cells (aka. contention zones), which are assumed to be the emerging and incumbent services, respectively. All cells share a single wide-band channel, and use CSMA/CA type of MAC channel access procedures specified in [1], [2], [5]. Each LAA and WLAN cell is controlled by an SBS and AP, respectively, or called scheduler in general, using LBT or distributed coordination function (DCF) protocols to sense the channel activity of other cells and schedule downlink transmissions. The system model is presented in Fig. 1, where each LTE-LAA SBS or WLAN AP senses channels and schedules downlink transmission to its associated users. Each user receives downlink ICIs of neighboring SBSs and APs, shown in red lines.

Let all cells be indexed by  $c \in \{1, \dots, C_{\text{tot}}\}$ , where  $C_{\text{tot}} = C_L + C_W$ ,  $c \in \{1, \dots, C_L\}$  refers to an LAA cell, and  $c \in \{C_L + 1, \dots, C_{\text{tot}}\}$  refers to a WLAN cell. There are  $N_c$  users in cell  $c$ , and pair  $(c, n)$  denotes user node  $n$  in cell  $c$ . The downlink transmit power at cell  $c$  is denoted as  $P_{T,c}$ .

Throughout this paper, we use subscripts  $L, W, I, S, F$ , and  $P$  to denote LAA, WLAN, idle, successful transmission, failed transmission, and payload, respectively. For cell  $c$ , we define  $\delta$ ,  $T_{P,c}$ ,  $T_{S,c}$  and  $T_{F,c}$  as durations of idle slot, payload, successful transmission, and failed transmission, respectively;

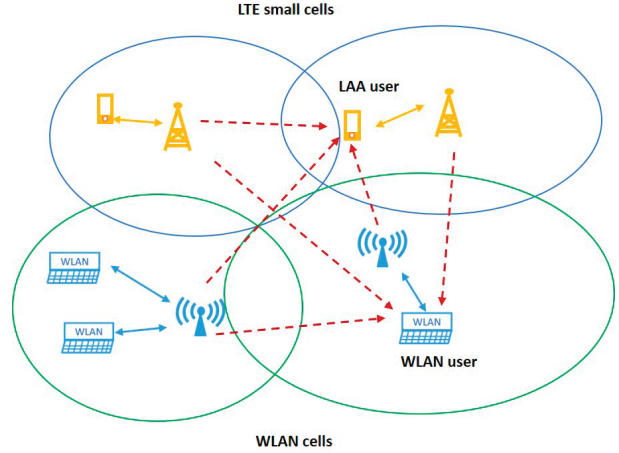


Fig. 1: Model of multi-cell LTE-LAA and WLAN systems.

and define  $\tau_c$ ,  $P_{I,c}$ ,  $P_{S,c}$  and  $P_{F,c}$  as the probabilities of channel access, channel idle, successful transmission, and failed transmission.

We consider a frequency-flat Rayleigh block fading channel model for each communication and interference link, which is static in a block of milli-seconds level (which approximately corresponds to a transmission duration), then changes independently from block to block. The power of channel gain from scheduler  $c_2$  to user  $(c, n)$  is denoted as  $h_{(c,n),c_2}$ , and the power of channel from scheduler  $c_2$  to scheduler  $c$  is represented as  $g_{c,c_2}$ . The probability density function (PDF) of channel power  $h_{(c,n),c_2}$  is given by

$$h_{(c,n),c_2}(P) = \exp(-P/\bar{P})/\bar{P}, \quad (1)$$

where  $\bar{P}$  is the average power of fading channel gain. Based on [18], we have  $\bar{P} = E[h_{(c,n),c_2}] = (4\pi/\lambda_c)^2 d_{(c,n),c_2}^{-\alpha_d}$ , where  $\lambda_c$  is the carrier wavelength,  $d_{(c,n),c_2}$  is distance between scheduler  $c_2$  to node  $(c, n)$ , and  $\alpha_d$  is the path loss exponent.

Regarding the MAC parameters at scheduler  $c$ , we assume that the contention window size (CWS) is  $W_{c,m}$  at backoff stage  $m$  (for  $m = 0, 1, \dots, M_c$ ), where  $M_c$  is the maximum backoff stage. We present the SCA and ECA schemes next.

### Multi-cell Downlink SCA Scheme:

Each scheduler  $c$  implements the following procedure:

- 1) Based on a CSMA/CA protocol, scheduler  $c$  draws an initial backoff counter value within  $(0, W_{c,m} - 1)$  based on the current CWS  $W_{c,m}$ .
- 2) Scheduler  $c$  senses channel activities and compares the received sum ICI power with sensing threshold  $I_{d,c}$  during each sensing slot  $\delta$ .
- 3) If ICI power exceeds threshold, scheduler  $c$  freezes its backoff counter; otherwise, it reduces counter value by one. Go back to Step 2) when counter is larger than zero; otherwise go to step 4).
- 4) Based on either request-to-send/clear to send (RTS/CTS) or basic access, scheduler  $c$  sends handshaking or payload signals to associated users.
- 5) If the majority of transmissions are successful, scheduler  $c$  reduces CWS to  $W_{c,0}$ ; otherwise, it doubles the CWS,

unless the maximum CWS  $W_{c,M_c}$  is reached. Go back to step 1).

On the other hand, when the cells are highly overlapped spatially, and/or when the sensing threshold at every scheduler is very low, each scheduler can detect transmissions in any adjacent cell perfectly. We call this the Multi-cell Downlink ECA Scheduling Scheme.

To implement LBT or DCF, an SBS uses only one threshold based on energy detection (ED)  $I_{L,ed}$  to sense transmissions in other cells, and an AP uses two thresholds – carrier sensing (CS) threshold  $I_{W,cs}$  to sense WLAN transmissions of other cells, and ED threshold  $I_{W,ed}$  to detect other type of transmissions (such as LAA signals), respectively. We use  $I_{d,c,c_2}$  to denote the sensing threshold of scheduler  $c$  to detect signals from a neighboring cell  $c_2$ , then

$$I_{d,c,c_2} = \begin{cases} I_{L,ed} & \text{for } c \in \{1, \dots, C_L\}, \text{ and any } c_2, \\ I_{W,ed} & \text{for } c \in \{C_L + 1, \dots, C_{tot}\}, \\ & \text{and } c_2 \in \{1, \dots, C_L\} \\ I_{W,cs} & \text{for } c \in \{C_L + 1, \dots, C_{tot}\}, \\ & \text{and } c_2 \in \{C_L + 1, \dots, C_{tot}\}. \end{cases}$$

Furthermore, we define  $I_{f,c}$  as the ICI maximum tolerance threshold at scheduler  $c$ .

### III. PERFORMANCE ANALYSIS

We first derive the multi-cell LAA and WLAN coexistence performance with the SCA, and then simplify the results to the ECA and discuss their relationship.

#### A. Shared Cell Access

In this method, we model the ICI from each source individually, and then combine the impacts. We use  $\hat{H}_0$  and  $\hat{H}_1$  to denote decisions of null and transmission, respectively. We define  $P_{d,c,c_2}$  as the detection probability of scheduler  $c_2$  at scheduler  $c$ , when a transmission from cell  $c_2$  with power  $P_{T,c_2}$  starts, with decision threshold  $I_{d,c,c_2}$  and local noise power spectrum density (PSD)  $N_{0,c}$ . Thus,

$$P_{d,c,c_2} = \Pr(P_{T,c_2}g_{c,c_2} + N_{0,c} < I_{d,c,c_2}).$$

Suppose that we use a sensing duration of  $\delta_{SS}$  with sampling rate  $B_W$ , and obtain  $[\delta_{SS}B_W]$  samples to make a block decision, where  $[x]$  rounds  $x$  to its nearest integer. By default,  $\delta = 9 \mu s$  and  $\delta_{SS} \geq 4 \mu s$  at the 5 GHz ISM band [2], [5]. Typically,  $\delta_{SS}B_W \gg 1$  holds. For example, when  $\delta_{SS} = 5 \mu s$  and  $B_W = 20$  MHz, we have  $[\delta_{SS}B_W] = 100$ . With  $\delta_{SS}B_W \gg 1$ , the sum power of the sampled complex noise has a Gamma distribution with degree of freedom (DOF)  $[2\delta_{SS}B_W]$ , which approximates a constant. On the other hand, due to limited Doppler shift for small-cell communication, we model the inter-SBS/AP channel  $g_{c,c_2}$  as a slow Rayleigh fading channel, and its DOF is only 2 in the  $\delta_{SS}$  sensing duration. In summary, the magnitude of the received ICI follows a Rayleigh distribution in the  $\delta_{SS}$  duration (slow fading), and its power follows an exponential distribution.

We obtain the inter-cell detection probability as

$$\begin{aligned} P_{d,c,c_2} &= \Pr(P_{T,c_2}g_{c,c_2} < \tilde{I}_{d,c,c_2}) \\ &\simeq 1 - \exp(-\tilde{I}_{d,c,c_2}/[P_{T,c_2}\bar{g}_{c,c_2}]), \end{aligned} \quad (2)$$

where  $\tilde{I}_{d,c,c_2} = \max(I_{d,c,c_2} - N_{0,c}, 0)$ ,  $\bar{g}_{c,c_2} = E[g_{c,c_2}]$ , and  $E[\cdot]$  here is with respect to the fading channel distribution.

Furthermore, we define  $P_{f,c,c_2}$  as the probability that ICI from cell  $c_2$  causes transmission of cell  $c$  to fail. We obtain that  $P_{f,c,c_2} = \Pr(P_{T,c_2}g_{c,c_2} < \tilde{I}_{f,c}) \simeq 1 - \exp(-\tilde{I}_{f,c}/[P_{T,c_2}\bar{g}_{c,c_2}])$ , where  $\tilde{I}_{f,c} = \max(I_{f,c} - N_{0,c}, 0)$ .

Define  $\tilde{P}_{suc,c}$  as the conditional STP of scheduler  $c$  when its transmission starts, and  $P_{suc,c}$  as the average STP. We obtain  $\tilde{P}_{suc,c} = \prod_{c_2=1}^{C_{tot}} (1 - \tau_{c_2} P_{f,c,c_2})$ . Note that in  $\tilde{P}_{suc,c}$  the term  $1 - \tau_{c_2} P_{f,c,c_2}$  can be decomposed to two parts:  $1 - \tau_{c_2}$  which is probability that cell  $c_2$  is not active and  $\tau_{c_2}(1 - P_{f,c,c_2})$ , which is probability that cell  $c_2$  is active but its generated ICI does not cause transmission of cell  $c$  to fail.

The CAP of scheduler  $c$  is a function of  $\tilde{P}_{suc,c}$ ,  $W_{c,0}$ , and  $M_c$ . Based on [15], the CAP of scheduler  $c$  is given by:

$$\tau_c = \frac{2(1 - (1 - \tilde{P}_{suc,c})^{M_c+1})}{\tilde{P}_{suc,c} \sum_{j=0}^{M_c} (1 - \tilde{P}_{suc,c})^j (1 + W_c)}. \quad (3)$$

We derive the average STP at cell  $c$  as

$$P_{suc,c} = \tau_c \tilde{P}_{suc,c}. \quad (4)$$

We define  $T_{suc,c,n}$  as the normalized throughput duration (NTD) of user  $(c, n)$ , which is given by

$$T_{suc,c,n} = \alpha_{(c,n)} P_{suc,c} T_{P,c} / T_{ave,c},$$

where  $\alpha_{(c,n)}$  is time ratio allocated to node  $n$  (with  $\sum_{n=1}^{N_c} \alpha_{(c,n)} = 1$ ), and  $T_{ave,c}$  is the average time in cell  $c$  to support one successful transmission. The overall NTD at cell  $c$  is given by

$$T_{suc,c} = \sum_{n=1}^{N_c} T_{suc,c,n}. \quad (5)$$

The NTD is conceptually similar to the successful channel occupancy efficiency, or called normalized throughput in [15]–[17]. Note that  $\sum_{c=1}^{C_{tot}} T_{suc,c} > 1$  can hold for the SCA scheme, but not for the ECA scheme. The NTD does not model the physical-layer data rate.

To model both MAC- and physical-layer features, we define the average throughput of user  $(c, n)$  as

$$\begin{aligned} S_{c,n} &= \alpha_{(c,n)} P_{suc,c} T_{P,c} \\ &\cdot B_{(c,n)} E[\log_2(1 + \beta_{(c,n)} \gamma_{(c,n)})] / T_{ave,c}, \end{aligned} \quad (6)$$

where  $\gamma_{(c,n)}$  is the signal-to-interference-and-noise ratio (SINR) at user  $(c, n)$ ,  $E[\cdot]$  is the expectation with respect to the distribution of  $\gamma_{(c,n)}$ , and  $\beta_{(c,n)}$  is the signal-to-noise ratio (SNR) gap function [18], given by  $\beta_{(c,n)} = -1.5 / \log(5\text{BER}_{(c,n)})$ , where  $\text{BER}_{(c,n)}$  is the target bit error rate (BER) for user traffic. The cell  $c$  sum-throughput is given by

$$S_c = \sum_{n=1}^{N_c} S_{c,n}. \quad (7)$$

We derive  $\gamma_{(c,n)}$  as

$$\gamma_{(c,n)} = \frac{P_{T,c} h_{(c,n),c}}{I_{tot,(c,n)}(\hat{H}_0) + N_{0,c}}, \quad (8)$$

where  $I_{\text{tot},(c,n)}(\hat{H}_0)$  is the average total interference power at node  $(c,n)$  under  $\hat{H}_0$  decision at cell  $c$ , when the scheduler  $c$  starts a downlink transmission. It is given by

$$I_{\text{tot},(c,n)}(\hat{H}_0) = \sum_{\substack{c_2=1 \\ c_2 \neq c}}^{C_{\text{tot}}} P_{T,c_2} \tau_{c_2} \bar{h}_{(c,n),c_2} (1 - P_{d,c,c_2}). \quad (9)$$

where  $\bar{h}_{(c,n),c_2} = E[h_{(c,n),c_2}]$ . In (9), we introduce the factor  $(1 - P_{d,c,c_2})$  to represent the probability of experienced ICI at scheduler  $c$ .

Finally, we analyze the  $T_{\text{ave},c}$  which is challenging to evaluate due to the multi-cell ICIs and CCA errors. To distinguish between LAA and WLAN cells, we use  $T_{F,L}$  and  $T_{F,W}$  to denote durations caused by failed transmission in an LAA and WLAN cell, and  $T_{F,M} = \max(T_{F,L}, T_{F,W})$ . After some manipulations, we derive  $T_{\text{ave},c}$  as

$$T_{\text{ave},c} = P_{I,c} \delta + P_{\text{suc},c} T_{S,c} + \sum_{\substack{c_2=1 \\ c_2 \neq c}}^{C_{\text{tot}}} P_{d,c,c_2} P_{\text{suc},c_2} T_{S,c_2} + P_{F,L,c} T_{F,L} + P_{F,W,c} T_{F,W} + P_{F,LW,c} T_{F,M}, \quad (10)$$

where the first, second and third terms are related to events of system idle, successful transmission at cell  $c$ , and cell- $c$  sensed successful transmissions of other cells, respectively; and in the 4th to 6th terms  $P_{F,L,c}$ ,  $P_{F,W,c}$ , and  $P_{F,LW,c}$  are, respectively, probabilities of failed transmissions (e.g. caused by collisions) at only LAA cells, at only WLAN cells, and at both LAA and WLAN cells. In detail,  $P_{I,c}$  is the system idle probability sensed by scheduler  $c$ , given by

$$P_{I,c} = \prod_{c_2=1}^{C_{\text{tot}}} (1 - \tau_{c_2} P_{d,c,c_2}), \quad (11)$$

where  $P_{d,c,c} = 1$  holds. In the 3rd term of (10), the factor  $P_{d,c,c_2}$  models an important fact that scheduler  $c$  only freezes its counter when it can sense a downlink transmission in cell  $c_2$ . We can combine the second and third terms to  $\sum_{c_2=1}^{C_{\text{tot}}} P_{d,c,c_2} P_{\text{suc},c_2} T_{S,c_2}$  by using the fact that  $P_{d,c,c} = 1$  holds. Furthermore, we can obtain that in (10),

$$P_{F,L,c} = \left[ \prod_{c_2=C_L+1}^{C_{\text{tot}}} (1 - \tau_{c_2} P_{d,c,c_2}) \right] \cdot \left[ 1 - \prod_{c_2=1}^{C_L} (1 - \tau_{c_2} P_{d,c,c_2}) - \sum_{c_2=1}^{C_L} P_{d,c,c_2} P_{\text{suc},c_2} \right] \quad (12)$$

$$P_{F,LW,c} = \left[ 1 - \prod_{c_2=1}^{C_L} (1 - \tau_{c_2} P_{d,c,c_2}) \right] \cdot \left[ 1 - \prod_{c_2=C_L+1}^{C_{\text{tot}}} (1 - \tau_{c_2} P_{d,c,c_2}) \right], \quad (13)$$

where on the right handside of (12), the first factor models the probability of failed transmission event at LAA cells, and the second factor is the probability of idle channel event at WLAN cells, when both events happen and are sensed by scheduler  $c$ . The expression of  $P_{F,W,c}$  can be obtained using a similar

procedure, but is omitted here due to the space limitation.

When  $T_{F,L} = T_{F,W} = T_F$  holds, we can simplify (10) to

$$T_{\text{ave},c} = P_{I,c} \delta + \sum_{c_2=1}^{C_{\text{tot}}} P_{d,c,c_2} P_{\text{suc},c_2} T_{S,c_2} + P_{F,c} T_F,$$

where

$$\begin{aligned} P_{F,c} &= P_{F,L,c} + P_{F,W,c} + P_{F,LW,c} \\ &= 1 - P_{I,c} - \sum_{c_2=1}^{C_{\text{tot}}} P_{d,c,c_2} P_{\text{suc},c_2}. \end{aligned} \quad (14)$$

The novelty of our method can be briefly explained as follows: Our method is more accurate than several state-of-the-art results on modeling LBT MAC features and the impact of inter-SBS/AP ICI sensing errors. For example, [7]–[9], [12] did not model the CSMA/CA multistage backoff and/or average time to support one successful transmission, see (10). Furthermore, the provided throughput formulas in [7]–[13] did not explicitly address imperfect ICI sensing and its impact of KPIs. More generally, from the open literature we have not found validated multi-cell multi-tier KPI results for coexistence systems (such as LAA and WLAN) that flexibly take into account both CSMA/CA LBT MAC procedures and CCA sensing errors. These issues have been addressed in this paper. We show in Subsection III-B that our SCA result simplifies to that of ECA when the inter-cell detection probability approaches unity, and is equivalent to known results. In Section IV, we further provide Monte Carlo simulation results to validate the analysis.

## B. Exclusive Cell Access

The ECA can be modeled by assuming perfect sensing  $P_{d,c,c_2} = 1$  for all  $c$  and  $c_2$ . Certainly, this assumption is only valid for special cases, such as a region of highly overlapped cells, high transmission powers, and/or very sensitive sensing thresholds.

The average throughput at user  $(c,n)$  is given in the form of (6), but with the following changes: the  $\tau_c$ ,  $\tilde{P}_{\text{suc},c}$ ,  $P_{\text{suc},c}$ ,  $\gamma_{(c,n)}$  and  $T_{\text{ave},c}$  therein shall be changed by replacing  $P_{d,c,c_2} = 1$  therein. Then we obtain

$$\tilde{P}_{\text{suc},c}^{\text{ECA}} = \prod_{\substack{c_2=1 \\ c_2 \neq c}}^{C_{\text{tot}}} (1 - \tau_{c_2}),$$

$P_{\text{suc},c}^{\text{ECA}} = \tau_c \tilde{P}_{\text{suc},c}^{\text{ECA}}$  and  $\gamma_{(c,n)}^{\text{ECA}} = \frac{P_{T,c} h_{(c,n),c}}{N_{0,c}}$ . Note that the SINR  $\gamma_{(c,n)}$  in the SCA scheme becomes the SNR in the ECA scheme since ICI is avoided due to perfect inter-cell sensing.

To gain insight into LAA and WLAN coexistence, we assume that the  $C_L$  LAA cells have homogeneous CSMA/CA parameters, and so are the  $C_W$  WLAN cells. We also write the CAP, the idle, successful transmission, and failed transmission probabilities of all the LAA (or WLAN) cells as  $\tau_L$ ,  $P_{I,L}$ ,  $P_{S,L}$ , and  $P_{F,L}$  (or  $\tau_W$ ,  $P_{I,W}$ ,  $P_{S,W}$ , and  $P_{F,W}$ ), respectively.

Under assumptions of perfect sensing and ECA, we obtain:

$$\begin{aligned}
P_{I,L} &= \prod_{c=1}^{C_L} (1 - \tau_{c,L}), \\
P_{S,L} &= \sum_{c=1}^{C_L} \tau_{c,L} \left[ \prod_{\substack{c_2=1 \\ c_2 \neq c}}^{C_L} (1 - \tau_{c_2,L}) \right], \\
P_{F,L} &= 1 - P_{I,L} - P_{S,L}.
\end{aligned}$$

When all SBS nodes have homogenous MAC parameters, i.e.,  $\tau_{c,L} = \tau_L$  for all  $c$ , we obtain:

$$\begin{aligned}
P_{I,L} &= (1 - \tau_{c,L})^{C_L}, \\
P_{S,L} &= C_L \tau_{c,L} (1 - \tau_{c,L})^{C_L - 1},
\end{aligned}$$

and  $P_{F,L} = 1 - P_{I,L} - P_{S,L}$ . Similarly,  $P_{I,W} = (1 - \tau_{c,W})^{C_W}$ ,  $P_{S,W} = C_W \tau_{c,W} (1 - \tau_{c,W})^{C_W - 1}$ , and  $P_{F,W} = 1 - P_{I,W} - P_{S,W}$ .

Furthermore, (10) is simplified to

$$\begin{aligned}
T_{\text{ave}}^{\text{ECA}} &= P_I^{\text{ECA}} \delta + P_{\text{suc},L}^{\text{ECA}} T_{S,L} + P_{\text{suc},W}^{\text{ECA}} T_{S,W} \\
&\quad + P_{F,L}^{\text{ECA}} T_{F,L} + P_{F,W}^{\text{ECA}} T_{F,W} + P_{F,LW}^{\text{ECA}} T_{F,M}, \quad (15)
\end{aligned}$$

where  $P_I^{\text{ECA}} = P_{I,L} P_{I,W}$ ,  $P_{\text{suc},L}^{\text{ECA}} = P_{I,W} P_{S,L}$ ,  $P_{\text{suc},W}^{\text{ECA}} = P_{I,L} P_{S,W}$ ,  $P_{F,L}^{\text{ECA}} = P_{I,W} P_{F,L}$ ,  $P_{F,W}^{\text{ECA}} = P_{I,L} P_{F,W}$ , and  $P_{F,LW}^{\text{ECA}} = (1 - P_{I,L})(1 - P_{I,W})$ . We can show that (15) is equivalent to a result given by eq. (19) in [15], when the latter is reduced from three transmission types to two types.

#### IV. NUMERICAL RESULTS

In this section, we provide both analytical and simulation results to validate our analysis, and show impact of critical parameters such as the sensing thresholds.

We develop a new simulator by using a constant simulation step-size (aka, event update interval) of an idle slot duration  $\delta$  to track the effect of sensing error event. All schedulers (aka. SBSs and APs) follow multi-cell LBT procedures. We assume a slow fading channel, and the sensing result at each scheduler is updated when any transmission in the system starts or stops. The simulator tracks all the backoff, transmission, and sensing error events, and computes average KPIs.

Some CSMA/CA parameters and equations to compute  $T_{S,L}$  (and  $T_{F,L}$ ) from  $T_{P,L}$ , and to compute  $T_{S,W}$  (and  $T_{F,W}$ ) from  $T_{P,W}$  are provided in [16]. Assume that there are  $N_L$  (or  $N_W$ ) users in each LAA (or WLAN) cell, with CWS  $W_{L,0}$  (or  $W_{W,0}$ ), and maximum backoff stage  $M_L$  (or  $M_W$ ), respectively. Unless otherwise stated, we assume that  $\alpha_d = 3.5$ ,  $\delta = 9\mu\text{s}$ , total area has a rectangle shape with size  $R_0 \times R_0$ , and each cell has a disk shape with radius  $r_0$ . Further, we assume carrier frequency  $f_c = 5.2$  GHz,  $P_{T,c} = 23$  dBm,  $B_{(c,n)} = 20$  MHz,  $\text{BER}_{(c,n)} = 10^{-3}$ ,  $\alpha_{(c,n)} = 1/N_c$  for all  $c$  and  $n$ , and background white Gaussian noise has PSD of -174 dBm/Hz. RTS/CTS is used for both LAA and WLAN cells. To model the effects of minimum link distance and limited modulation size, the SNR or SINR per link is truncated to 20 dB as an upper-bound. We choose these physical and MAC parameters to represent a feasible multicell coexistence scenario.

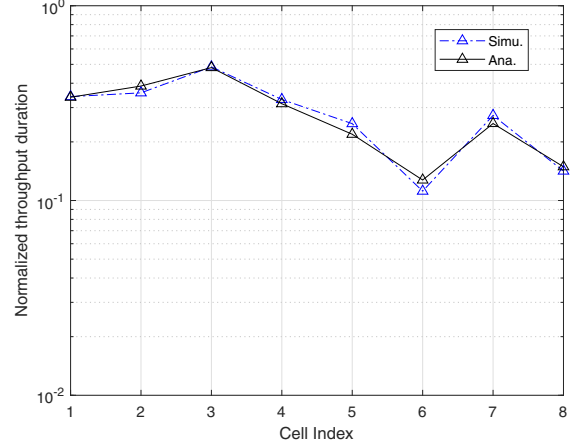


Fig. 2: Normalized cell-throughput duration of the LTE-LAA and WLAN system vs. cell index, and the first and next 4 cells are LAA and WLAN cells, respectively.

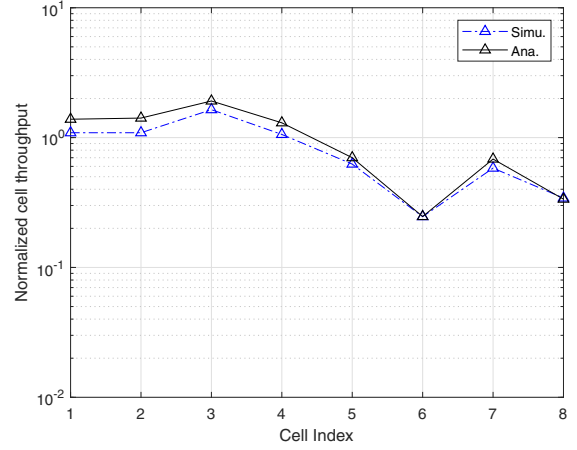


Fig. 3: Normalized cell throughput of the LTE-LAA and WLAN system vs. cell index, with the same system setting as for Fig. 2.

We provide analytical and simulation results on the per-cell NTD based on eq. (5) in Fig. 2, and throughput based on eq. (7) but normalized by the channel bandwidth in Fig. 3. For both figures, we assume that  $N_L = N_W = 5$ ,  $W_{L,0} = 8$ ,  $W_{W,0} = 16$ ,  $M_L = M_W = 1$ ,  $I_{f,c} = I_{d,c} = -72$  dBm for all  $c$ ,  $T_{P,W} = T_{P,L} = 10\delta$ ,  $R_0 = 100$  m, and  $r_0 = 30$  m. We ran the algorithms for  $2 \times 10^4$  time slots to obtain the average statistics. Due to random locations of SBSs, APs and users, the NTDs and normalized throughputs among the cells are heterogeneous. Figs. 2 and 3 illustrate consistent matching among analytical and simulation results, which account for effects of ICI and sensing errors. The minor mismatch between simulation and analytical results in Fig. 3 is likely caused by the difficulty of analytically evaluating the distribution of the sum ICIs experienced by each user when packets are received. This issue will be addressed in our future work.

Next, we show analytical numerical results on normalized

## V. CONCLUSION

In this paper, we have modeled and analyzed the KPIs of LBT-related multi-cell 2-tier coexisting systems (LTE-LAA and WLAN), and provided a unified analysis of the multi-cell SCA and ECA schemes as function of detection probability and sensing thresholds. We have programmed an idle-slot step-size event-update simulation tool to better track sensing error events and provided reliable simulation results to verify our analysis. Numerical results demonstrate effects of various MAC and system parameters, such as LAA and WLAN sensing thresholds, and show that SCA with proper threshold setting provides significantly greater cell sum throughput than the ECA scheme. This result provides powerful analytical and simulation tools for performance evaluation of multi-tier coexistence systems with imperfect sensing, and supports system optimization in a practical way.

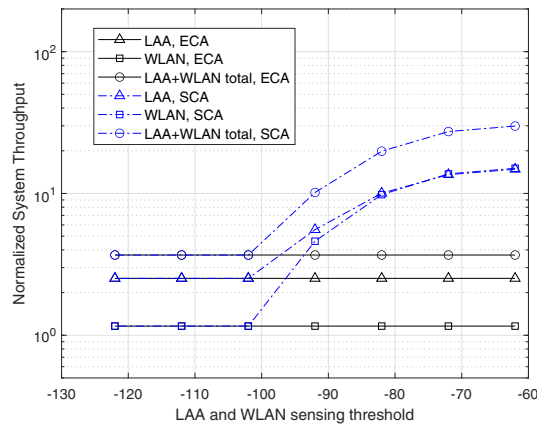


Fig. 4: Normalized system throughput of the LTE-LAA and WLAN systems vs. LAA and WLAN sensing threshold.

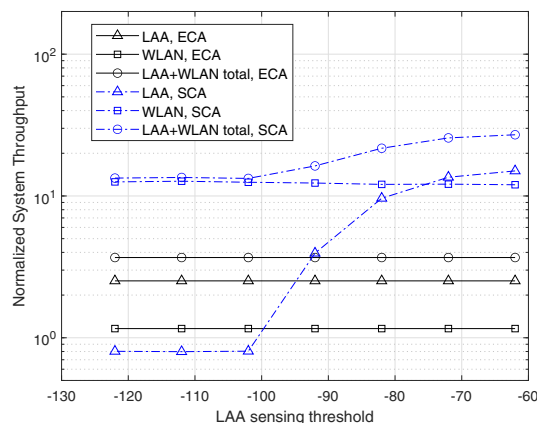


Fig. 5: Normalized system throughput of the LTE-LAA and WLAN systems vs. only LAA sensing threshold.

system throughput vs. sensing thresholds in Fig. 4 and Fig. 5, respectively, assuming  $C_L = C_W = 6$ ,  $N_L = N_W = 5$ ,  $W_{L,0} = W_{W,0} = 16$ ,  $M_L = 1$ ,  $M_W = 4$ ,  $I_{L,ed} = -72$  dBm,  $I_{W,cs} = -82$  dBm,  $I_{W,ed} = -62$  dBm,  $T_{P,W} = T_{P,L} = 1$  ms,  $R_0 = 200$  m and  $r_0 = 30$  m. The results were obtained by averaging over 1000 random location profiles.

For Fig. 4, we assume that all LAA and WLAN sensing thresholds are equal and vary between  $[-122, -62]$  dBm. Fig. 4 verifies that when all sensing thresholds are reduced to about  $-102$  dBm or lower (from the right to the left), the throughputs of the SCA scheme (LAA and WLAN) are reduced significantly and converge to those of the ECA scheme, as expected, because the inter-SBS/AP detection probabilities approach unity in this example. Fig. 5 provides throughput vs. LAA sensing threshold  $I_{L,ed}$  which varies in the range of  $[-122, -62]$  dBm, but WLAN sensing thresholds are fixed. We observe that when LAA SBSs reduce their sensing threshold from  $-62$  dBm to  $-102$  dBm, the LAA throughput reduces significantly from about 15 to 0.8, but the WLAN throughput is insensitive to the LAA threshold change.

## REFERENCES

- [1] 3GPP TSG RAN, "Study On Licensed-Assisted Access To Unlicensed Spectrum", 3GPP TR 36.889 V13.0.0, Jun. 2015.
- [2] 3GPP TS RAN, "E-UTRA Physical layer procedures (Release 14)", 3GPP TS 36.213 V14.4.0, Sept. 2017.
- [3] 3GPP TSG RAN, "Study on NR-based access to unlicensed spectrum", 3GPP TR 38.889 V16.0.0, Dec. 2018.
- [4] A. Mukherjee et al., "Licensed-assisted access LTE: coexistence with IEEE 802.11 and the evolution toward 5G," *IEEE Commun. Mag.*, vol. 54, no. 6, pp. 50-57, Jun. 2016.
- [5] IEEE LAN/MAN Standards Committee, IEEE Std 802.11-2012, Part 11: Wireless LAN Medium Access Control (MAC) and Physical Layer (PHY) Specifications, Feb. 2012.
- [6] L. Dai and X. Sun, "A unified analysis of IEEE 802.11 DCF networks: stability, throughput, and delay," *IEEE Trans. Mobile Computing*, vol. 12, no. 8, pp. 1558-1572, Aug. 2013.
- [7] Y. Li, F. Baccelli, J. G. Andrews, T. D. Novlan and J. C. Zhang, "Modeling and analyzing the coexistence of Wi-Fi and LTE in unlicensed spectrum," *IEEE Trans. Wireless Commun.*, vol. 15, no. 9, pp. 6310-6326, Sept. 2016.
- [8] X. Wang, T. Q. S. Quek, M. Sheng and J. Li, "Throughput and fairness analysis of Wi-Fi and LTE-U in unlicensed band," *IEEE J. Sel. Areas Commun.*, vol. 35, no. 1, pp. 63-78, Jan. 2017.
- [9] C. Liu and H. Tsai, "On the limits of coexisting coverage and capacity in multi-RAT heterogeneous networks," *IEEE Trans. Wireless Commun.*, vol. 16, no. 5, pp. 3086-3101, May 2017.
- [10] N. Rastegardoost and B. Jabbari, "Minimizing Wi-Fi latency with unlicensed LTE opportunistic white-space utilization," *IEEE Trans. Wireless Commun.*, vol. 18, no. 3, pp. 1914-1926, March 2019.
- [11] G. Bianchi, "Performance analysis of the IEEE 802.11 distributed coordination function," *IEEE J. Sel. Areas Commun.*, vol. 18, no. 3, pp. 535-547, Mar. 2000.
- [12] R. Yin, G. Yu, A. Maaref, and G. Li, "A framework for co-channel interference and collision probability tradeoff in LTE licensed-assisted access networks," *IEEE Trans. Wireless Commun.*, vol. 15, no. 9, pp. 6078-6090, Sept. 2016.
- [13] S. Han, Y. C. Liang, Q. Chen and B. H. Soong, "Licensed-assisted access for LTE in unlicensed spectrum: A MAC protocol design," *IEEE J. Sel. Areas Commun.*, vol. 34, no. 10, pp. 2550-2561, Oct. 2016.
- [14] Y. Song, K. W. Sung, and Y. Han, "Coexistence of Wi-Fi and cellular with listen-before-talk in unlicensed spectrum," *IEEE Commun. Lett.*, vol. 20, no. 1, pp. 161-164, Jan. 2016.
- [15] Y. Ma and D. G. Kuester, "MAC-layer coexistence analysis of LTE and WLAN systems via listen-before-talk," in *Proc. IEEE CCNC*, Las Vegas, NV, 2017, pp. 534-541.
- [16] Y. Ma, D. G. Kuester, J. Coder and W. F. Young, "Slot-jamming effect and mitigation between LTE-LAA and WLAN systems with heterogeneous slot durations," *IEEE Trans. Commun.*, vol. 67, no. 6, pp. 4407-4422, June 2019.
- [17] Y. Ma and J. Coder, "Analysis of generalized CCA errors and mitigation in LTE-LAA spectrum sharing system," *Proc. IEEE GlobeCom*, Hawaii, USA, Dec. 2019, pp. 1-7.
- [18] A. Goldsmith, *Wireless Communications*, Cambridge University Press, 2005.